7th International Conference on Fatigue Design, Fatigue Design 2017, 29-30 November 2017, Senlis, France

Modeling fatigue behavior of slewing rings in crane structures. Identification of influencing parameters on local stresses and fatigue damage calculations

R. Duval[a] *, M. Bennebach[a], J. Blasiak[b], A. Guelbi[b]

aCETIM, 52 Avenue Felix Louat, 60304 Senlis cedex, France
bMANITOWOC, 66 chemin du Moulin Carron, 69570 Dardilly, France

Abstract

In the case of Crane industry sector, with high requirements of security and performance, slewing rings are important parts of equipment and manufacturers need to guarantee their mechanical strength and durability. Since more than ten years, on demand of industrial groups, CETIM is working on slewing rings in the fields of tests, design and calculations.

For the last couple of years, extensive work has been done to develop a calculation methodology giving access to forces in balls of rings. These forces, used as input of local non-linear finite element models including contact definition, allow stress state calculations in tracks of rings. Fatigue analysis is then conducted based on appropriate criteria taking into account the complex multiaxial stress state and the gradient of material properties due to the surface treatment of the tracks (induction hardened parts). Parametric calculations have been made in order to estimate the influence of some parameters such as contact angle of the balls, geometric conformity, mechanical clearance and depth of treated material. Results allow identifying most important parameters and show how these parameters influence the damage location on the slewing rings, with good correlation with physical observations on damaged components. A synthesis of this long term work is presented in this paper.

* Corresponding author. Tel.: +33-3-44-67-32-94 ; fax: +33-3-44-67-32-90.
E-mail address: romain.duval@cetim.fr

1. Introduction

From 1997 to 2015, CETIM worked together with industrial partners in order to develop robust methodologies dedicated to slewing rings design [1, 2, 3].

Before 2005, studies focused on slewing rings assemblies. Exhaustive tests and calculations have been performed resulting in a general method for designing slewing ring assembly. This work has led to software tool called Cetim-PEARL.

To calculate the assembly, a force by sector is needed. Until 2005, a formula assuming perfect sinusoidal repartition has been used to calculate forces in balls. From 2005 to 2010, a methodology based on finite element method has been developed to calculate accurately the repartition of ball forces around slewing ring. This methodology uses nonlinear springs to simulate contact. It's necessary to use this method when stiffness of support structure is not uniform. Section 3 of this paper presents this calculation method.

Force and contact angle calculated from the previous global approach are then used as input to a local finite element model which considers nonlinear contact between ball and track. The stress state in tracks is calculated with this model, presented in section 4.

Once calculated the stress field in the tracks, corresponding to a realistic loading sequence, a fatigue analysis may be carried out thanks to an appropriate fatigue criterion. In order to take into account the complex multiaxial stress state involved in such case (contact fatigue), the Dang Van criterion was used. Section 5 describes the model.

Force in ball calculation, local contact finite element model together with fatigue analysis are influenced by parameters such as initial contact angle, geometric conformity, diameter gap or hardening treatment thickness. Section 6 gives a global overview of the parametric analysis.

Nomenclature

D_{mean} : Mean ring diameter [m]

D_{ball} : Ball diameter [m]

Z : Number of balls

α : Contact angle

$M_{bend.}$: Bending moment [N.m]

F_{axial} : Axial force [N]

ψ : Relative rotation angle between inner and outer rings [°]

---

2. Slewing ring description

2.1. Definition and geometry

The slewing ring considered in this paper is a member of a tower crane as shown on Figure 1. It guides rotation of jib (horizontal beam). This slewing has one balls row and can be globally described by the following parameters:

- $D_{mean} = 1410\ mm$
- $D_{ball} = 45\ mm$
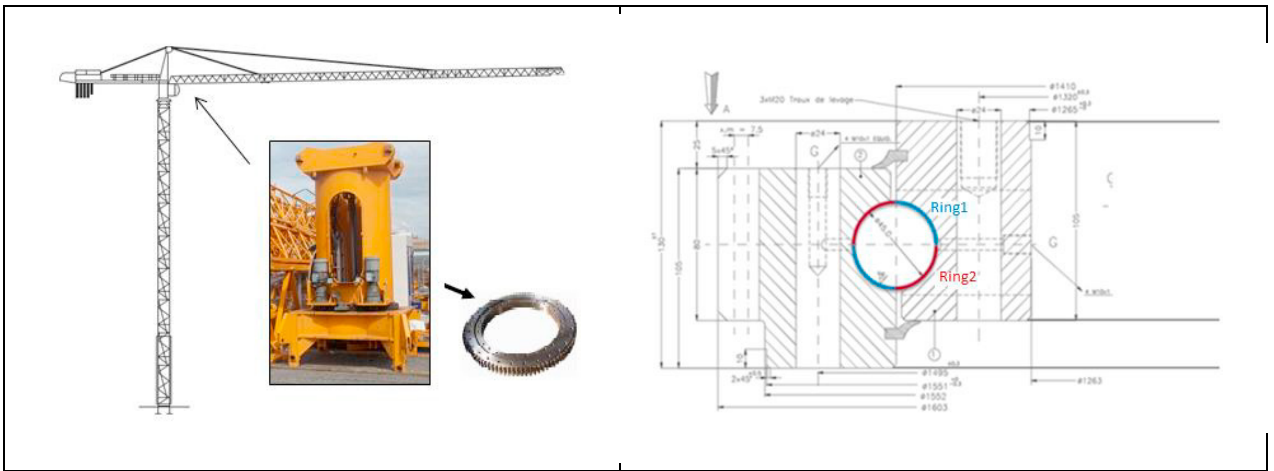
- $Z = 87$
- $\alpha = 45°$

Figure 1 : Slewing ring position on the tower crane

Material is a quenched and tempered steel grade 42CrMo4 and track is induction hardened through a thickness of 3,2 mm.
Difference in curvature between ball and track is given by a parameter called geometric conformity, which is defined by the ratio of track radius over ball diameter.

2.2. Global loading cycle

For the service condition cycle considered, jib rotates counter clockwise carrying a load and comes back clockwise without load, over an angle of 180°. Figure 2 shows graphically this cycle.
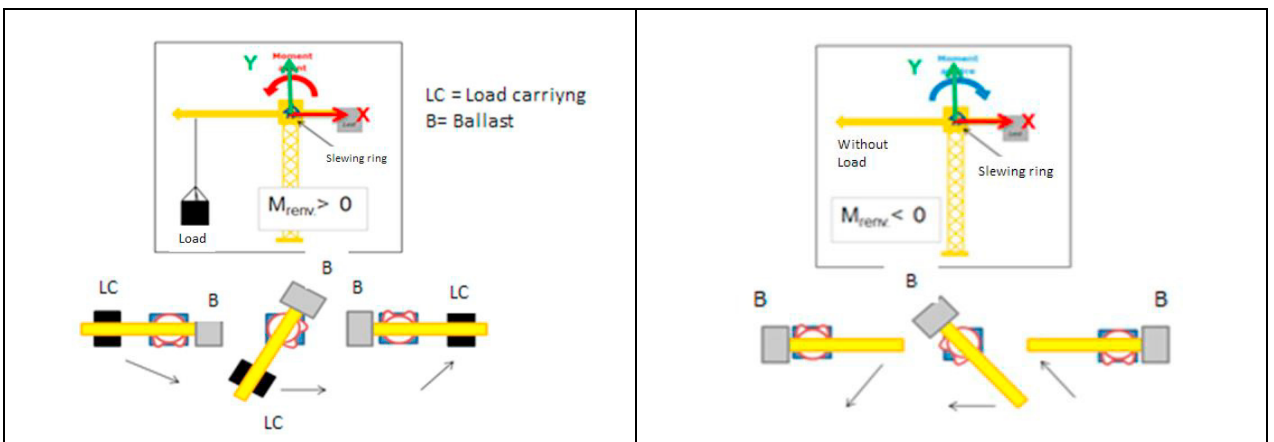

Figure 2 : Loading cycle (Left = With Load; Right = Without Load)

2.3. Local loading cycle

When jib turns, inner and outer rings rotate with a relative angle of ψ. As rings move, balls roll, and a point on the track sees a local cycle when a ball passes. The number of local cycles can be calculated giving contact angle, ball diameter, mean ring diameter, rotation angle and number of balls. Equation (1) gives the number of local cycles for moving ring (+) and fixed ring (-).

$$N_{local\ cycle} = \frac{Z}{360} * \frac{\psi}{2} * \left(1 \pm \frac{D_{ball}*\cos(\alpha)}{D_{mean}}\right) \tag{1}$$

One ring is fixed and the other is turning. The fixed ring sees a load that moves together with jib. Depending on jib angular position, the loaded sector is different. The moving ring moves together with jib; the loaded sector does not depend of jib position. Moving ring has two critical sectors, one near lest and the other at the opposite side.

3. Ball force and contact angle calculation [4, 5]

Considering rigid rings, no clearance and a number of balls higher than 26, maximum force in balls can be calculated giving slewing rings geometry, number of balls and global loading with the following equation:

$$F_{eq} = \frac{1}{\sin(\alpha)} \times \left(\frac{\frac{4 \times M_{bend.}}{D_{mean}} \pm F_{axial}}{Z}\right) \tag{2}$$

The ring and support structure on which ring is fixed are not rigid. Some sectors are more rigid than others. Equation (2) considers a uniform stiffness. When a ball passes on a flexible sector, force is less than expected; while when it passes on a stiff sector, force is more than expected. In order to calculate real forces, work has been done to include flexibility of supporting parts in calculation model.

3.1. Global assembly

First, supporting structures are created and loaded (cf. Figure 3). The turntable is fixed at its four feet. Axial force and bending moment (cf. Figure 2) are applied on top of carrier through a remote point. Calculation is done with load and then without load. Four positions are considered at 0°, 15°, 30° and 45°. Loads follow carrier's rotation. Thanks to turntable's double symmetry, it's not necessary to calculate positions from 60° to 180°.
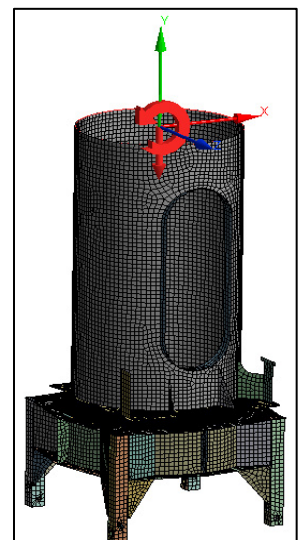

Figure 3 : Slewing ring, carrier and turntable meshes and loading (at 0°)

3.2. Contact model

To simulate ball's stiffness and contact, a nonlinear spring links center of curvature of opposite tracks. Its nonlinear stiffness curve and equation are given in Figure 4.

The equation shown in the figure:

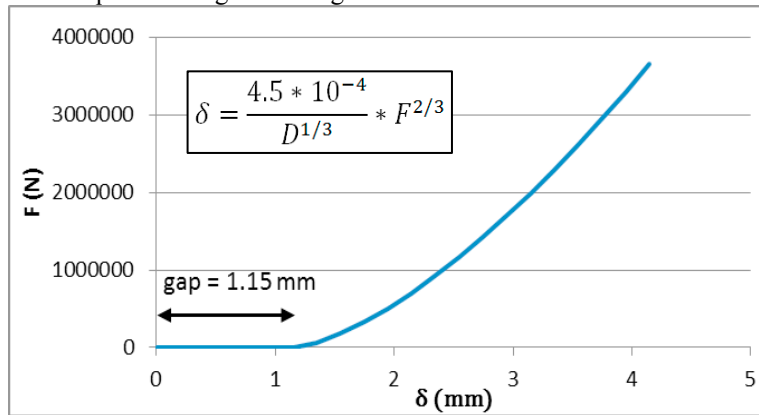$$\delta = \frac{4.5 * 10^{-4}}{D^{1/3}} * F^{2/3}$$

gap = 1.15 mm

Figure 4 : Spring nonlinear stiffness

When the slewing ring gets loaded or when a gap exists, contact angle changes. This contact angle is given by spring's contact angle. Figure 5 shows spring in the diagonal (top left / bottom right). When load sign is changed, diagonal changes (bottom left / top right). Another spring is created in this diagonal.
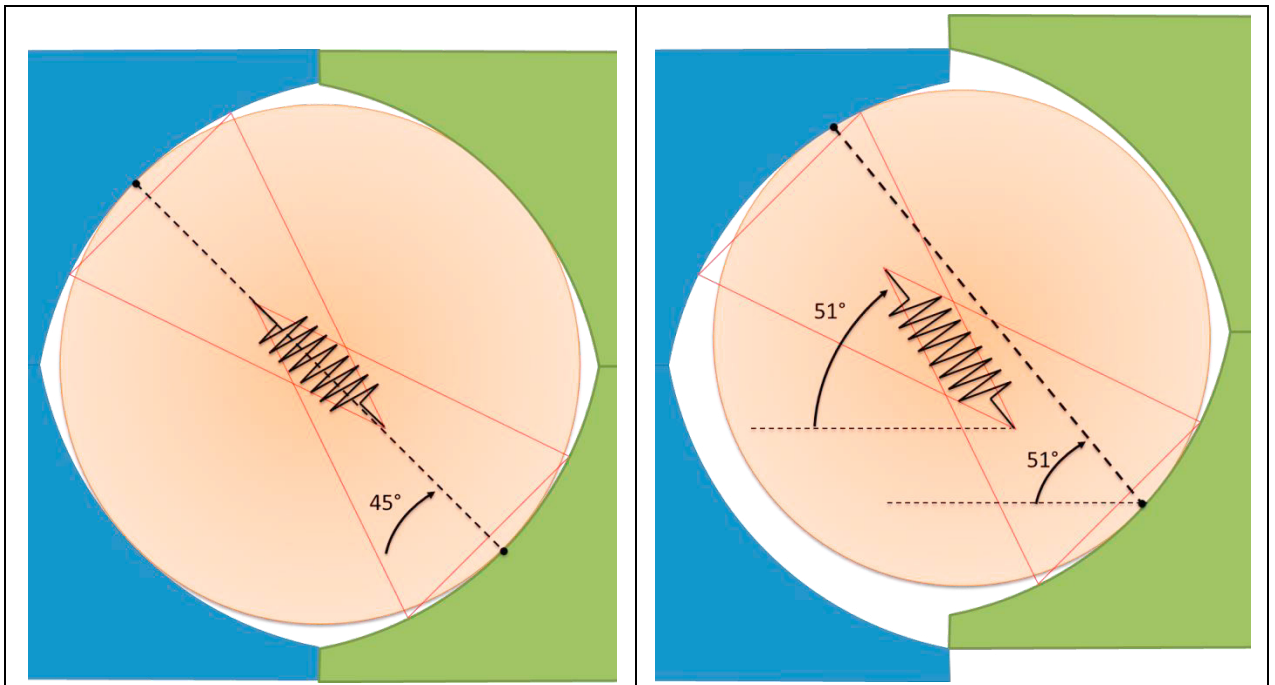

Figure 5 : Rigid beams and spring (contact angle = 45° and 51°)

Rigid beams are created from track's face to center of curvature. These beams are then linked with multi points constraints (MPC) to underlying elements (cf. Figure 6).
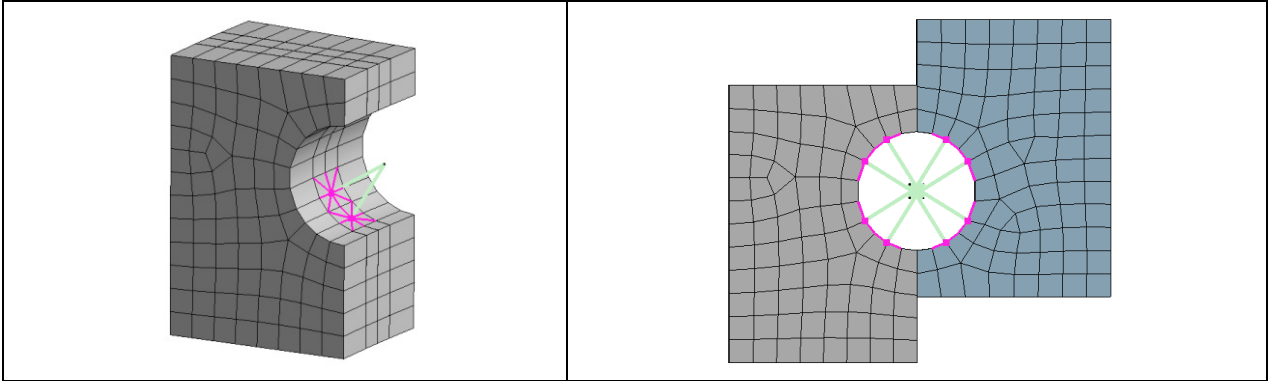
Figure 6 : Rigid beams (green) and MPC (purple)

Main result of this model is forces and contact angles in balls over 360°. As shown on Figure 7 and Figure 8, force in balls (here vertical component) vary from ideal sinusoidal repartition (difference of 25% on Figure 8).
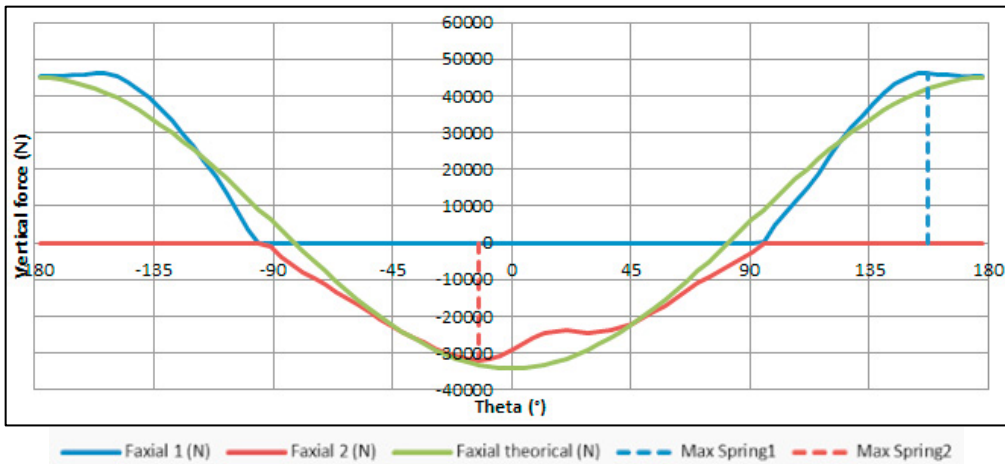

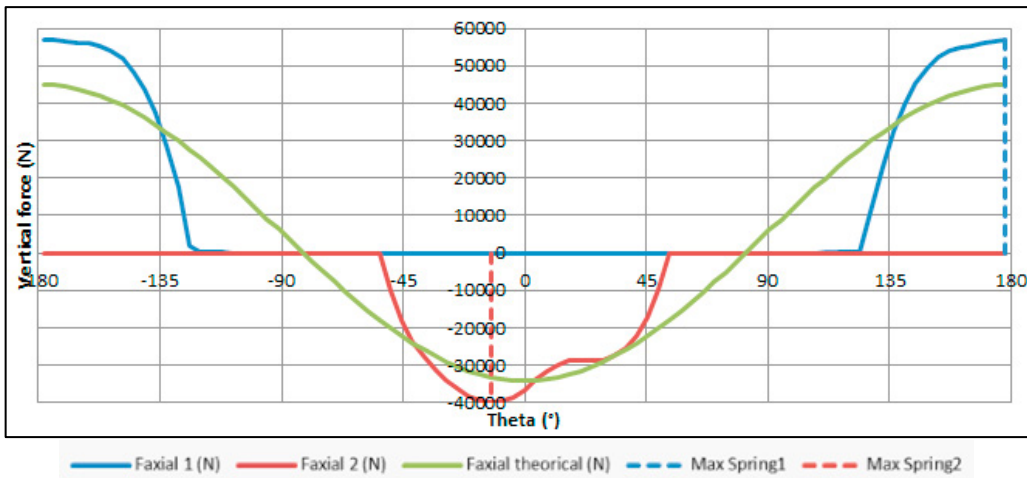Figure 7 : Vertical forces in balls (initial parameters, no gap)

Figure 8 : Vertical forces in balls (initial parameters, with 1,146 mm gap)

4. Finite element local model with non-linear contact

The model developed in section 3 gives local forces and angles. Critical ball sector is chosen and a local model is created, with symmetry considered. Two positions of ball are considered in order to charge top and bottom tracks. Model uses 3D solid elements. On the contact area, meshes between ball and track are coincident to give best stress results on surface. Figure 9 shows a schematic summary of this local model.
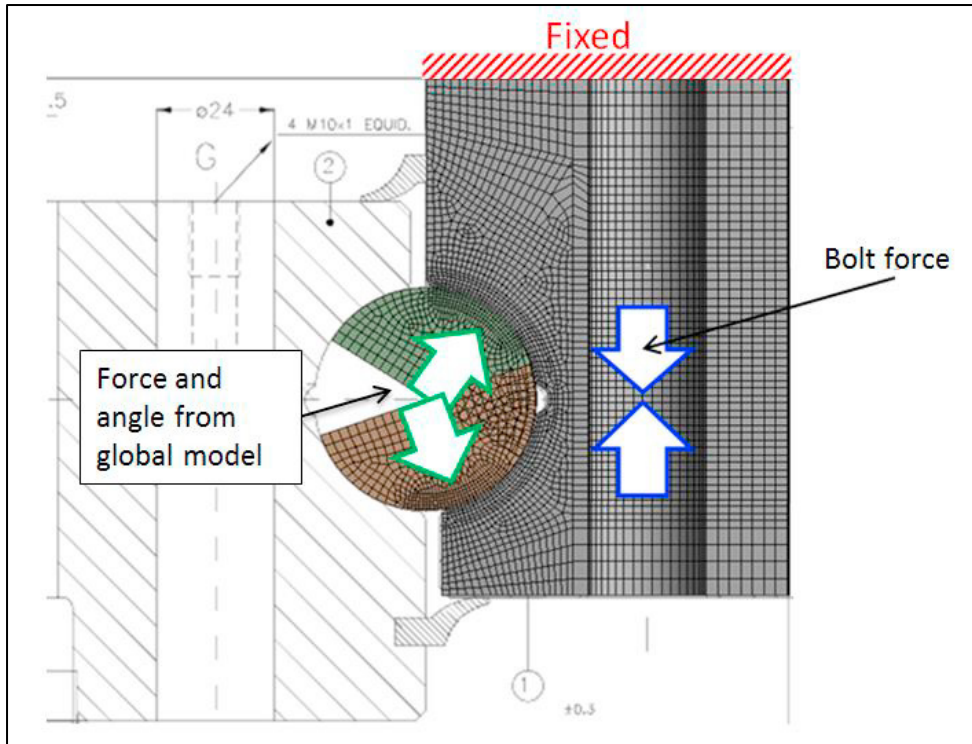

Figure 9 : Local finite element model

5. Fatigue analysis

Local stresses calculated from the local model described section 4 are used in a fatigue damage assessment. The multiaxial fatigue Dang Van criterion is applied [6]. This criterion aims to deal with high cycle fatigue conditions where the damage occurs at a microscopic level. The formulation uses the current local values of shear stress $\tau(t)$ and hydrostatic pressure $p(t)$ to calculate an "equivalent" stress and compare it to a threshold. No damage will occur if:

$$\tau(t) + a.p(t) \le b, \forall t \in T \qquad (3)$$

a, b are material parameters calculated from two simple fatigue tests
T is the loading period.

The relation between the macroscopic stresses $\Sigma_{ij}(t)$ and the microscopic ones $\sigma_{ij}(t)$ is given by:

$$\sigma_{ij}(t) = \Sigma_{ij}(t) + \rho_{ij}^{*} \qquad (4)$$

ρ_{ij}^{*} being the stabilized local residual stress tensor, calculated by means of an iterative process in which convergence assumes a state of elastic shakedown. As it is proportional to the microscopic plastic strains, this tensor is a deviatoric.

The microscopic hydrostatic pressure is then equal to the macroscopic one:

$$p(t) = P(t) = 1/3 * \text{trace} \ [\Sigma_{ij}(t)] \tag{5}$$

The same relation applies to the deviatoric stresses:

$$s_{ij}(t) = S_{ij}(t) + \rho_{ij}^{*} \tag{6}$$

From the work of Papadopoulos, Dang Van proposed in 1987 to take $\rho_{ij}^{*} = -z_{ij}^{*}$, z_{ij}^{*} being the center of the smallest hypersphere that encompasses the path described by the macroscopic deviatoric stress tensor $S_{ij}(t)$. It is in fact the solution of the min-max problem :

$$z_{ij}^{*} : \min_{z_{ij}} \ \left\{ \ \max_{t} \ \sqrt{(S_{ij}(t) - z_{ij}) : (S_{ij}(t) - z_{ij})} \ \right\} \tag{7}$$

Once ρ_{ij}^{*} is calculated, the local shear stress $\tau(t)$ is determined from the microscopic deviatoric stresses using the Tresca criterion.

A safety factor can then be calculated as:

$$SF = \frac{b}{\max(\tau(t) + a \times p(t))} \tag{8}$$

The Dang Van criterion is a threshold type model, locating a stress path with regard to an endurance threshold, as illustrated figure 10.
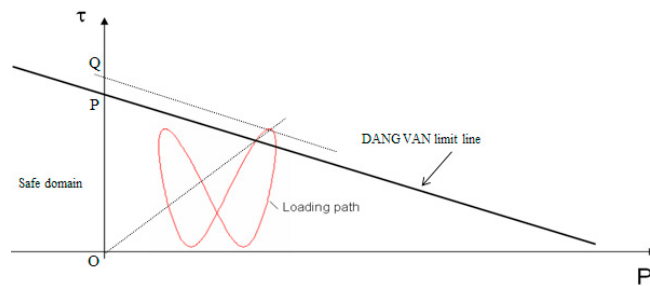

Figure 10 : Sample Dang Van diagram

The parameters used for the tracks base metal and hardened section are respectively given equations (9) and (10). These are estimates from ultimate tensile strength, sufficient for the comparisons made section 6.

$$\tau(t) + 0{,}35.p(t) = 430 \ \text{(Induction hardened)} \tag{9}$$

$$\tau(t) + 0{,}35.p(t) = 330 \ \text{(Base metal)} \tag{10}$$

The estimated thresholds correspond to endurance domain (~10^6 cycles).

6. Parametric analysis results

In addition to the reference model presented in section 2, five other models with different parameters have been studied. A small design of experiments (D.O.E.) is conducted in order to evaluate sensitivity of results under parameters variation. Let's recall that the parameters investigated are: treatment thickness, initial contact angle, geometric conformity and diameter gap. All investigated configurations are listed in table 1.

Table 1 : Configurations studied

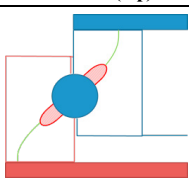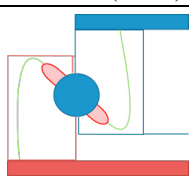|	Case 0 (reference)	Case 1	Case 2	Case 3	Case 4	Case 5
Treatment thickness [mm]	3,2	4,5	3,2	3,2	3,2	3,2
Initial angle [°]	45	45	50	45	45	45
Track / ball conformity	0,522	0,522	0,522	0,511	0,522	0,58
Diameter gap* [mm]	0	0	0	0	1.146	1.146

6.1. Global model results

Due to strong influence of the gap parameter compared to other parameters, D.O.E. is separated in two: without gap (cases 0 to 3) and with gap (cases 4 and 5).

6.1.1. Without gap

Results (force and angle) are listed in Table 2.

Table 2 : D.O.E. results – Cases without gap

	Parameters				**Global model results**					
					Track 1 (top)			**Track 2 (bottom)**		
	Thick. [mm]	Ang. [°]	Conf. [-]	Gap [mm]	Fmax1 normal	Fmax1 axial	Angle1	Fmax2 normal	Fmax2 axial	Angle2
Case 0	3.2	45	0.522	0	68604	55852	54.5	38269	35330	67.4
Case 1	4.5	45	0.522	0	68604	55852	54.5	38269	35330	67.4
Case 2	3.2	50	0.522	0	66107	55379	56.9	37812	35532	70
Case 3	3.2	45	0.511	0	65492	55419	57.8	38119	37327	78.3

Case 0 : reference

For this reference case, contact angle on track 2 (bottom) is high (67°). Force on track 1 (top) is bigger than on track 2 but contact angle remains near 45° thanks to track 1 stiffness. Track 2 has a smaller stiffness resulting in a contact

angle of 67°. This weakness is due to the ring part geometry that has less material behind track 2 than behind track 1. Furthermore, force on track 2 generates in plane bending; while on track 1, it goes directly in fixed support.

Case 1 : Treatment thickness

Not use in global model. Will be considered in fatigue analysis.

Case 2 : Initial angle of 50° (reference = 45°)

On track 1, initial contact angle of 50° reduces slightly the forces. Contact angle remains near 45°.
On track 2, this change increases contact angle to 70° and has to be avoided.
An initial contact angle of 50° could be considered on track 1 which is stiff but not on track 2 which has less stiffness.

Case 3 : Conformity of 0,511 (reference = 0,522)

Increase of conformity has a negative effect on track 1 and 2 because it increases contact angle. However, effect should be analyse on stresses later because Hertzian stress should be less with a conformity near 0,5.
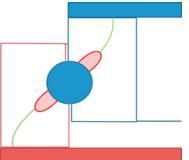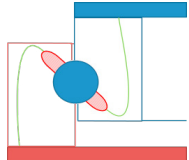In cases 1 to 3, investigated parameters were design parameters. Observations above can then be use at design stage. However, some parameters are not controlled and have to be evaluated. Gap is a non-controlled parameter that tends to augment when slewing ring is used. Next two cases show gap influence and how conformity can counterbalance its effect.

6.1.2. With gap

Results (force and angle) are listed in Table 2.

Table 3 : D.O.E. results – Cases with gap

	Parameters			Global model results						
				Track 1 (top)			Track 2 (bottom)			
	Thick. [mm]	Ang. [°]	Conf. [-]	Gap [mm]	Fmax1 normal	axial	Angle1	Fmax2 normal	axial	Angle2
Case 0	3.2	45	0.522	0	68604	55852	54.5	38269	35330	67.4
Case 4	3.2	45	0.522	1.146	73014	65901	64.5	44598	43158	75.4
Case 5	3.2	45	0.58	1.146	81014	66605	55.3	44959	38778	59.6

Case 4 : Gap of 1.146 mm

When gap is present, fewer balls are in contact. Therefore, balls in contact get more force. As shown in Figure 5, gap increases initial contact angle. On track 2, contact angle is 75°. This has to be avoided because it has been shown that fatigue failure occurs in that area of the tracks. Fatigue analysis in section 6.2 confirms this point.

Case 5 : Gap of 1.146 mm and conformity of 0.58 (reference =0.522)

Increasing geometric conformity prevents from angle contact changes. Thanks to this change in conformity, case 5 (with gap) gives better results in terms of angles than reference case (without gap). If failures near tracks border are observed, a change in conformity can help.

Contact force seems to increase drastically of 18% (69kN to 81kN) but this increase is linked to the added gap (not controlled) that increases axial force. On case 4, this increase seems smaller but it is just because contact angle has changed to 65°.

Conformity can help to prevent change in angle but should be kept as low as possible because as conformity increases, contact geometry tends towards a ball on plane configuration instead of a ball on cylinder.

6.2. Fatigue analysis results

Table 2 summarizes fatigue results for investigated configurations.

Table 4 : Fatigue calculation results

	Case 0	Case 1	Case 2	Case 3	Case 4	Case 5
Treatment thickness [mm]	3,2	4,5	3,2	3,2	3,2	3,2
Initial angle[°]	45	45	50	45	45	45
Conformity	0,522	0,522	0,522	0,511	0,522	0,58
Diameter gap [mm]	0	0	0	0	1.146	1.146
Dang Van safety factor	0.97	0.97	0.98	0.65	0.53	0.68

The fatigue calculation, based on the Dang Van criterion, point out different possible failure locations according to the investigated case. Cases 0, 1 and 2 result in similar safety factors, with a behavior near endurance. Cases 3, 4 and 5 have to be avoided as they result in safety factors <<1. These configurations increase the fatigue failure risk.

In terms of failure locations, cases 2 and 4 present a high risk of failure at tracks border, in depth; for case 3 fatigue failure is predicted on the surface of the track.

Physical investigations on failed slewing rings tend to confirm these damage mechanisms.

7. Conclusion

Based on several years of collaborative work, Cetim in partnership with industrials developed a methodology dedicated to slewing rings design. This is based on a global model which results are used in a local calculation in order to obtain local stresses and then fatigue damage thanks to an appropriate criterion.

Results from a parametric analysis have been presented in this paper. It appears that:
- The treatment thickness, in the investigated depth range of 3.2 mm to 4.5 mm, has no real influence; critical points from computations being at a depth of less than 3.2 mm;
- Increasing the initial contact angle from 45° (reference) to 50° does not affect the level of damage compared to the chosen reference case. However, this increase of the angle makes appear a second critical zone, at the track border, with a non-negligible probability of failure.
- The reduction of conformity compared to the reference is penalizing in terms of fatigue damage. On the other hand, in this case a surface cracking is favoured, compared to the under layer cracks predicted in other cases.
- The most influential parameter is undoubtedly the diametric gap. The introduction of a gap with respect to the reference case (null gap), strongly reduces the fatigue strength and increases the risk of cracking in the track border. This parameter can be used as an indicator in the context of damage monitoring on the slewing ring.

Acknowledgements

References

[1] Simplified modeling of a slewing ring, L. Picot, M. Jubin, Cetim report n° 1J9004, 2007.
[2] Synthesis of studies on slewing rings, Z. Chaib, Cetim report n° 033835, 2010.
[3] Stress and fatigue analysis of slewing ring tracks, R. Duval, M. Bennebach, Cetim report n° 060396/060397, 2014.
[4] 3D Simplified Finite Elements Analysis of Load and Contact Angle in a Slewing Ball Bearing, A. Daidié, Z. Chaib, A. Ghosn, Journal of Mechanical Design, August 2008.
[5] Modeling and dimensioning of slewing rings, M. Henry, A. Guelbi, internal report, Manitowoc, 2012.
[6] On a new multiaxial fatigue limit criterion. Theory and application. K. Dang Van, B. Griveau, 0. Message, Biaxial and multiaxial fatigue, EGF3, Mechanical Engineering Publications, 1989.